Structurally-variable, rigid and optically-active D_2 and D_3 macrocycles possessing recognition properties towards C_{60}†

Carmine Coluccini,[a] Daniele Dondi,[b] Marco Caricato,[a] Angelo Taglietti,[b] Massimo Boiocchi[c] and Dario Pasini*[a]

Received 6th October 2009, Accepted 14th December 2009
First published as an Advance Article on the web 1st February 2010
DOI: 10.1039/b920867d

The reactivity of aromatic dicarboxylic acids, in combination with an axially-chiral, suitable dibenzylic alcohol, derived from BINOL, has been exploited in one-pot esterification reactions for the direct formation of several rigid, homochiral macrocycles. Cyclic adducts possessing, respectively, average molecular D_2 and D_3 symmetries, have been characterized in pure forms, with isolated yields and selectivities which are substantially different from those rising from purely statistical arguments. NMR and CD spectroscopies detect the structural and shape variability in the scaffolds, reflected both in terms of large changes in chemical shifts of selected proton resonances, and in terms of the variation of the CD signature related to the dihedral angle defined by the binaphthyl units embedded in the rigid cyclic skeleton. The crystal structure of two homochiral D_2 macrocycles show the formation of ordered nanostructures in the solid state, with the naphthyl rings of the binaphthyl units packing intermolecularly in an eclipsed-like conformation to yield nonhelical tubular arrangements. The larger D_3 cyclic adducts are able to afford stable complexes with C_{60} in toluene solution, with comparable binding strengths, yet whose stoichiometries are dependent on small variations in the spacing units and therefore in the shapes of the internal cavities of the cyclic structures.

Introduction

Large macrocyclic structures with a high degree of shape-persistency have been the subject of increasing interest for applications in the field of nanoscience.[1] The issue of conformational stability, and therefore rigidity, of the covalent cyclic structure is traditionally related to the possibility of enhancing the recognition/complexation properties towards suitable inclusion guests; more recently, however, this issue is stringent as one alternative target application of such rigid cycles is the formation *via* self-assembly of stable organic nanotubes by supramolecular organization in the third dimension. Different cyclic units, such as for example cyclic peptides,[2] phenylacetylene macrocycles,[3] amide-containing macrocycles,[4] or urea-based structures,[5] have been demonstrated to be useful for the above-mentioned objective. In all cases, the use of high-yielding, well established synthetic protocols for the rapid, covalent construction of the cyclic moieties is unavoidable.

Chiral self-assembled architectures continue to emerge as valuable building blocks for the design of various nanoscale assemblies with specific materials function as the desired output.[6] Given their robustness and their relative ease of derivatization BINOL (1,1′-binaphthyl-2,2′-diol) based synthons are becoming more and more attractive molecular modules for applications in fields spanning from asymmetric catalysis to materials science.[7] Macrocycles incorporating two or more BINOL units have already been proposed in the literature: Diederich *et al.* have reported the synthesis and supramolecular characterization of a number of large macrocycles, incorporating mainly 3 or 4 binaphthyl units such as (*R*)-**A**, *via* efficient Glaser coupling of the terminal acetylenic units introduced in the 3,3′ positions. The [2+2] macrocycle was not obtained, probably because the number of binaphthyl units required for closing the macrocycle is dictated, in the absence of flexible methylene carbon atoms, by the dihedral angle of the rigid binaphthyl unit.[8] Other strained [2+2] helical macrocycles have been obtained through Sonogashira coupling and incorporation of 6,6′-functionalized BINOL derivatives, such as (*R*)-**B**, and studied in terms of their peculiar properties as bent conjugated compounds.[9]

The subunit (*R*)-**C** has more recently been used, in conjunction with reductive amination protocols with aromatic diamines, for the construction of chiral macrocycles to be used as fluorescent enantioselective sensors for the detection of amino acids.[10] Conformationally flexible methylene carbon atoms (modulating the distortion derived by the incorporation in a cyclic structure of the axially-chiral units) are introduced in this case in the 3,3′ positions.

As part of a project dealing with chiral nanostructuring and nanotube formation, we have previously reported the rapid construction of BINOL-containing macrocycles by means of an esterification reaction in the cyclization step.[11] In this paper, we report on a generalization of this approach for the obtainment

[a]*Department of Organic Chemistry, University of Pavia, Viale Taramelli, 10 - 27100 - Pavia, Italy. E-mail: dario.pasini@unipv.it; Fax: (+39) 0382 987823; Tel: (+39) 0382 987835*
[b]*Department of General Chemistry, University of Pavia, Viale Taramelli, 10 - 27100 - Pavia, Italy*
[c]*Centro Grandi Strumenti, University of Pavia, Via Bassi, 21 - 27100 - Pavia, Italy*

† Electronic supplementary information (ESI) available: Additional crystallographic details, NMR spectra, titration experiments, atomic Cartesian coordinates of the calculated structures. CCDC reference numbers 746582 and 746583. For ESI and crystallographic data in CIF or other electronic format see DOI: 10.1039/b920867d

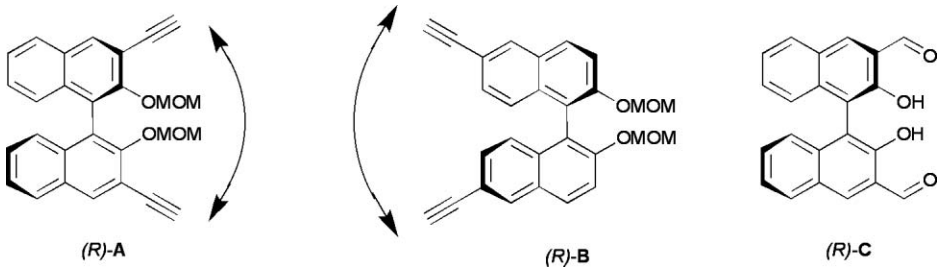

of novel chiral macrocyclic structures, on their solution and solid state characterization, and on their complexation properties towards C_{60}.

Results and discussion

Design, synthesis and NMR characterization

Our approach to the synthesis of flat, shape-persistent macrocycles containing binaphthyl units involve the introduction of rigid, aromatic spacers, and the use of an esterification reaction protocol. According to our design principles, the introduction of sp^3 carbon atoms, which impart a higher flexibility and conformational mobility to the covalent structure with respect to sp or sp^2 hybridized carbon atoms, has to be reduced to a minimum.[1b] However, their introduction is necessary to some extent in order to counterbalance the unavoidable bite angle introduced by the binaphthyl units, which would favour[8] larger, distorted, and non-ideally shaped macrocycles. Furthermore, the introduction of ester functionalities in the cyclization step could ensure both configurational and chemical stability to the resulting cyclic, covalent structure. In fact, in the light of the possible further noncovalent manipulation of the scaffold, the choice of an esterification approach instead of, for example, the widely used reductive amination approach,[10] avoids the incorporation of amines as basic, hydrogen-bonding competing sites in the cyclic framework.

The esterification is developed on the 3,3′ benzylic alcohol functionalities of the resolved derivative (*R*)-**1**[12] (Scheme 1), using a previously published esterification protocol. This protocol, originally developed by Moore and Stupp and reported to be highly efficient in the synthesis of aromatic polyesters,[13] and later used in the synthesis of dendrimers,[14] is based on the use of a carbodiimide coupling agent in the presence of stoichiometric amounts of the toluenesulfonic acid salt of DMAP (in general referred as DPTS), and applied, in the cited cases, in the presence of a minimum amount of reaction solvent. In the case of phthalic and terephthalic acid, both the [2+2] and the [3+3] macrocycles are obtained, possessing, respectively, average molecular D_2 and D_3 point group symmetries; the yields and selectivities of isolated products are unusual, especially considering that the [3+3] macrocycles are sometimes formed with equal synthetic efficiency to the [2+2] macrocycles, but in the former case there are six covalent bonds to be formed convergently in the cyclic structure (isolated yields are reported in Table 1). In all cases, the optimized reaction protocol was performed at intermediate dilution levels (each reagent 25 mM in CH_2Cl_2); attempts to reduce the concentration to 5 mM caused partial loss of reactivity, and reagents were not consumed after a 24 h period. In this optimized conditions, yields were substantially

Table 1 Yields of isolated cyclized products[a]

Entry	Diacid precursor	**3** (%)	**4** (%)
1[b]	**2a**	16	13
2	**2b**	10	3
3[b]	**2c**	18	9
4	**2d**	5	0
5	**2e**	0	0

[a] Isolated yield after column chromatography. For conditions, see Scheme 1 and discussion. [b] Data taken from ref. 11.

higher for all the monophenyl dicarboxylic acids (*ortho*, *para* or *meta*), with respect to 3,3′-diphenyl or 4,4′-diphenyl dicarboxylic acids; the 4,4′-disubstituted derivative **2e**, in fact, is completely insoluble in the solvent of the reaction (CH_2Cl_2), whereas all the others are sparingly soluble in this solvent. Attempts to use other protic or polar solvents (DMF, THF) in runs involving either **2c** or **2e** gave much worse results in terms of isolated yields, or no reactivity.

Alternative reaction methodologies were also briefly explored for comparison: by using the commercially available terephthaloyl chloride, fully soluble in CH_2Cl_2, at room temperature or reflux and in different dilution conditions (5 mM and 25 mM), the [2+2] adduct was detected in trace amounts and none of the [3+3] adduct could be detected, the remainder being polymeric, baseline material. These observations suggested the possible role as a template of one of the reagents or one of the by-products formed during the course of the reaction in the successful (DICD, DPTSA) conditions; however, ^{1}H NMR spectra (300 MHz, 10 mM in each component) of a 1 : 1 mixture of the [2+2] macrocycle **3c** or the [3+3] macrocycle **4c** and either DPTSA, DICD or an analogue of the urea reaction by-product (the commercially available diethyl urea) in $CDCl_3$, revealed no detectable shift in both the macrocyclic and the potential guest counterpart. Additional experiments aiming at verifying the possible thermodynamic reversibility of the esterification reaction protocol, run with the preformed macrocycle **3c** in the same concentration conditions (10 mM) and with the same reagent amounts used in its synthesis, revealed no scrambling of products (the formation also of **4c**), therefore excluding reactivity under thermodynamic control in a dynamic covalent manner.[15]

The room temperature ^{1}H NMR spectra for all cyclic compounds showed the expected simple patterns and the presence of only one set of signals for each group of symmetry-related proton resonances, revealing that all possible dynamic processes (slow rotation around the aryl–aryl bond in the case of **3d**, or conformational locking of the aromatic ester residues) are, as expected, fast on the NMR timescale at this temperature (see

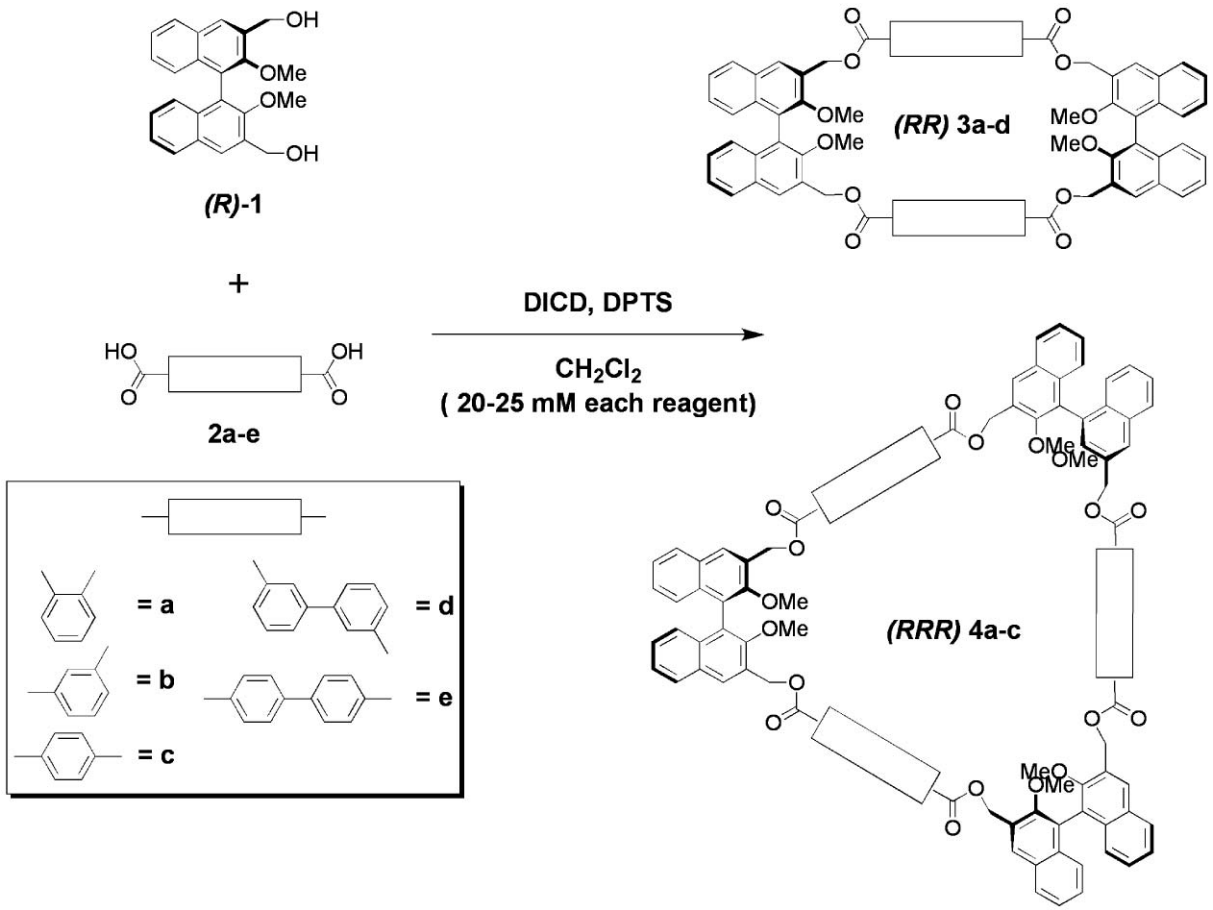

Scheme 1 Synthesis of key macrocycles **3** and **4**.

Figure S1†). It is interesting, however, to detect rather large differences in the chemical shift of the OMe groups proton resonances (Table S2,† from 2.88 ppm in the case of **3a** to 3.48 ppm in the case of **3c**); it is evident that while these functionalities experience a structurally-variable environment, induced by the presence of spacers of differing size, yet the covalent cyclic systems are able to maintain a high structural flexibility testified by the highly symmetrical ^{1}H NMR spectra at room temperature. Even more interestingly, in the case of *all* the D_3 macrocycles **4**, the CH_2 benzylic proton resonances appear as a collapsed AB system at room temperature, both at the 200 and the 300 MHz, as to demonstrate a peculiar, similar arrangement (within the class of the larger macrocycles) for the two diastereotopic methylene protons.[16] Thus, in the larger macrocycles these protons experience a local environment which is substantially different from that of the more rigid D_2 symmetrical analogues **3**, in which the methylene proton resonances appear as well defined and separated AB systems, suggesting the presence of flat preferred conformations in the case of the larger D_3 macrocycles (*vide infra*).

Crystal structures

Good quality crystals of macrocycles **3b** and **3c** could be obtained by slow evaporation of compounds from an acetone solution. The crystal and molecular structures have been obtained by X-ray diffraction studies of single crystals in which the macrocycles occur as acetone solvates. The molecular structures are shown as ORTEP plots in Fig. 1.

The **3b** macrocycle has no molecular symmetry and its cavity is not suitable to host any atom species; the **3c** macrocycle exhibits C_2 molecular symmetry and a cavity suitable to host the O atom of an acetone molecule. In both macrocycles the bonded naphthalene rings are placed accordingly to a perpendicular setting (dihedral angles between the naphthalene best plane are 76.8(2) and 84.9(2)° for **3b** and 77.7(2) and 84.7(2)° for **3c**). In **3b**, the two carbonyl oxygens of each *meta*-substituted aromatic ester spacers point towards opposite directions but the ester groups maintain an overall planarity with the connected aromatic ring: the displacement for the ester oxygens bonded to the C(2)–C(3)–C(4)–C(5)–C(6)–C(7) aromatic best plane are in the range –0.05(2) to +0.26(2) Å, whereas those bonded to the C(32)–C(33)–C(34)–C(35)–C(36) aromatic best plane are in the range –0.11(2) to +0.37(2) Å. Interestingly, the two aromatic esters of **3b** are placed almost perpendicularly, being the dihedral angle between the aromatic best plane 81.8(3)°. This arrangement combined with the "antisymmetrical" conformation of the C=O groups produces a loss of the D_2 molecular symmetry and in the solid state the **3b** macrocycle does not exhibit any molecular symmetry. All the geometrical features shown by the **3b** molecule correspond to a macrocycle in which the central cavity is occupied by atoms belonging to the macrocycle itself. Actually, two of the four methyl ether arms bonded to the binaphthyl moieties and two of the four

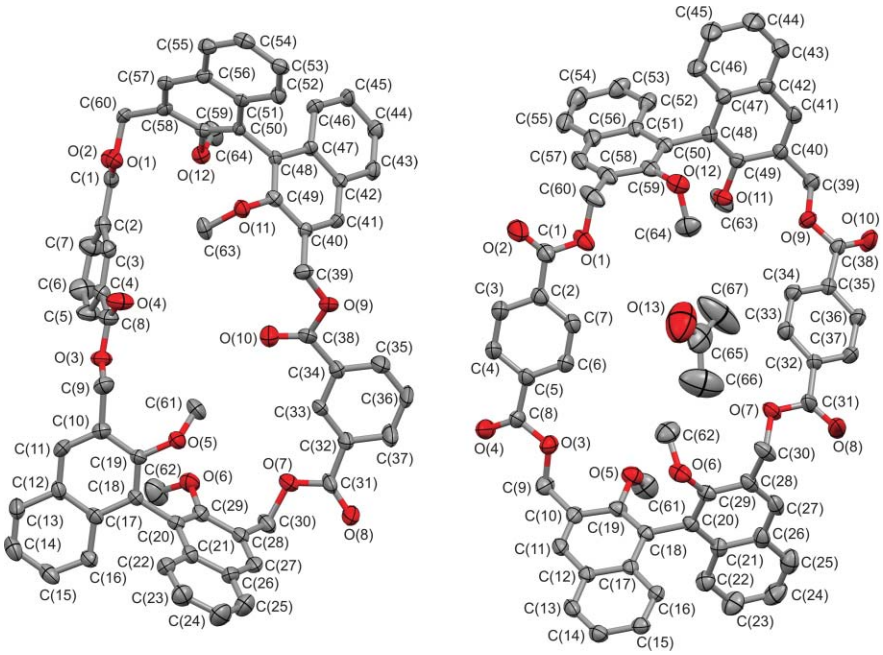

Fig. 1 ORTEP views of the **3b** (left) and **3c** (right) macrocycles (ellipsoids are drawn at the 30% probability level, H atoms have been omitted for clarity, as well as the two acetone solvent molecules for **3b** and one of the two acetone solvent molecules for **3c**).

carbonyl oxygens belonging to the aromatic ester arms point into the cavity, with one of the carbonyl oxygens [O(10)] placed only at 1.85(3) Å from the center of gravity of the overall molecule, which can be assumed as the center of the macrocycle cavity. Therefore the cavity of macrocycle **3b** in the crystal is unavailable to host other molecular groups. Also **3c** has the two *p*-substituted aromatic esters formed by almost planar atoms: the displacement for the ester oxygens bonded to the C(2)–C(3)–C(4)–C(5)–C(6)–C(7) aromatic best plane are in the range –0.29(1) to +0.44(1) Å, whereas those bonded to the C(32)–C(33)–C(34)–C(35)–C(36)–C(37) aromatic best plane are in the range –0.20(1) to +0.25(1) Å. However, each aromatic ester spacer is arranged with the two carbonyl oxygens pointing towards the same side and out of the macrocycle cavity. The aromatic rings of the two ester arms are also less perpendicular, the dihedral angle in **3c** being 50.6(2)°. All these features favour the partial maintenance of the ideal molecular symmetry and in the solid state the **3c** macrocycle exhibits C_2 molecular symmetry. Furthermore, the macrocycle cavity is longer than in **3b**: the measured distance between the centroid of the aryl–aryl bond of the two binaphthyl units of 12.62(1) Å for **3c** has to be compared with 11.89(1) Å for **3b**. The result is that atoms of the **3c** molecules are always placed at a distance longer than 2.83(2) Å from the center of gravity of the macrocycle, thus allowing for an acetone molecule to enter the cavity, placing its oxygen atom at 0.60(2) Å from the center of the cavity.

In the solid state, both molecules show a self assembling motif to form tubular structures. In particular, intermolecular contact shorter than the sum of the van der Waals radii has been observed for **3b** between the carbonyl O(8) atom of the aromatic ester spacers and the proton of the C(22) aromatic carbon of a naphthalene group belonging to an adjacent molecule. This suggest a weak C–H···O interaction that maintains the tubular structure. Probably a further C–H···O interaction occurs also for the O(4) carbonyl atom, which interacts with the proton of the C(43) aromatic carbon in a similar way but with a longer H···O distance (Fig. 2). Features of the C–H···O interactions are: C(22)···O(8) 3.22(2) Å, H(22)···O(8) 2.44(3) Å, C(22)–H(22)···O(8) 142.6(3)°; C(43)···O(4) 3.47(2) Å, H(43)···O(4) 2.74(3) Å, C(43)–H(43)···O(4) 135.4(3)°. The tubular structure extends along the *a* axis of the crystal and, as previously observed, it is mainly filled by the substituent groups connected to the macrocycle.

In the **3c** crystal, intermolecular contacts shorter than the sum of van der Waals radii occur between the ether O(12) atom and a proton of the CH_2 group of the C(9) atom. Therefore, also in this case it is a weak C–H···O interaction that maintains the columnar structure. Features of the C–H···O interaction are: C(9)···O(12) 3.12(2) Å, H(9a)···O(12) 2.31(2) Å, C(9)–H(9a)···O(12) 140.7(2)° (Fig. 3).

Although examples of the "serendipitous" formation of tubular structures in the solid state have been reported with achiral macrocyclic derivatives[17] and achiral cyclodextrin analogues,[18] these ordered solid-state polymers are unprecedentedly obtained with resolved, optically active macrocycles.

Spectroscopic and complexation studies

The UV/Vis absorption spectra of the macrocyclic compounds described in this paper show a band centered around 230 nm typical of the binaphthyl chromophore, with molar absorptivity values within the range of those already reported for this class of chromophores (5×10^4 to 10^5 M^{-1} cm^{-1} per binaphthyl chromophore in EtOH).[19a] Circular dichroism spectroscopy of macrocycles **3** and **4** shows the exciton couplet typical of binaphthyl moieties (Fig. 4), corresponding to the maximum absorption band in the UV/Vis spectra (*ca.* 230 nm for all compounds).

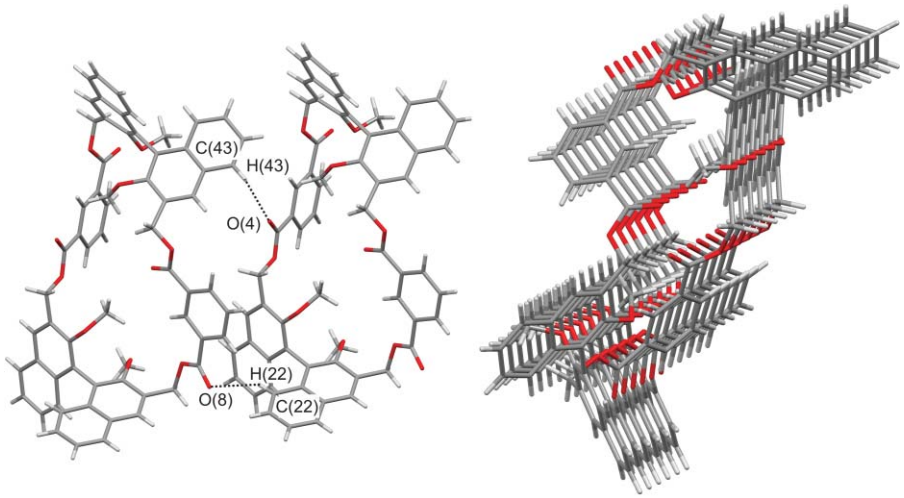

Fig. 2 A simplified sketch of the supramolecular solid state structure of **3b**. On the left is shown the intermolecular C–H···O motif that favours the formation of a columnar structure. On the right is shown the microtube that extends along the *a* crystallographic axis.

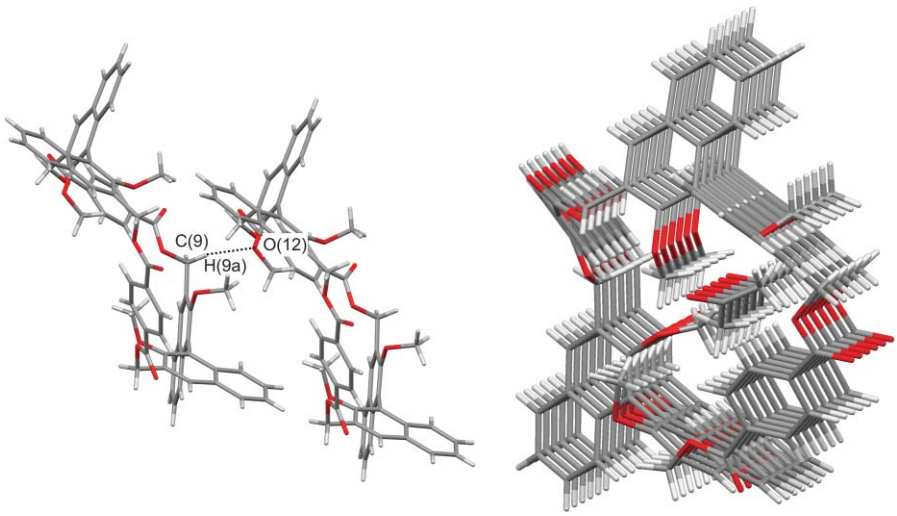

Fig. 3 A simplified sketch of the supramolecular solid state structure of **3c**. On the left is shown the intermolecular C–H···O motif that favours the formation of a columnar structure. On the right is shown the nanotube that extends along the *c* crystallographic axis and contains acetone solvent molecules.

The intensity of the low energy component of the couplet (at 230–240 nm) ranges between values of –120 for **3b** and –290 for **3d**; for O-substituted 2,2′-binaphthol derivatives, these values have been directly related to variations of the dihedral angle between the naphthyl units as a consequence of the steric hindrance of the substituents in the 2,2′-positions.[19b] Since compounds **3** possess the same substituent (OMe) in the 2,2′-positions, the differences between the above mentioned values should be ascribed to variations of the average dihedral angle of the binaphthyl units as a consequence of their incorporation in cyclic structures of differing sizes and structural flexibility, or, in other words, as a consequence of a more or less intense buttressing effect of the neighbouring 3,3′ benzylic ester positions.

The large internal cavities of shape-persistent macrocycles and the exploitation of concave–convex complementarity has resulted in several types of macrocyclic host molecules for C_{60} and higher fullerenes as guests. Planar aromatic π-electron extended surfaces, suitably positioned within a large covalent macrocyclic framework, have shown to be particularly effective in this context.[20] The observation that the cavities of the larger macrocycles (**4b**,**4c**) measure *ca.* 1 nm in size (*vide infra* molecular modeling), similarly to other shape persistent macrocycles which have already been reported to show recognition properties towards C_{60}, prompted us into investigating the complexation properties of these large rigid cycles towards C_{60}, carried out by UV/Vis spectroscopy.

By titrating a solution of C_{60} (5×10^{-5} M to 10^{-4} M) with increasing amounts of macrocycles **4b** and **4c** in toluene, a small but clearly detectable variation of the structure of the absorption band over 400 nm could be detected in both cases (Fig. 5 and 6). This band, arising with complex formation, is similar, both in terms of shape and intensities, to previously reported cases, involving both cyclic π-electron neutral and π-electron deficient substrates.[20c,e,l] In fact, the molar absorptivity values ε for complex formation (*e.g.* calculated in condition of saturation, and experimentally verified)

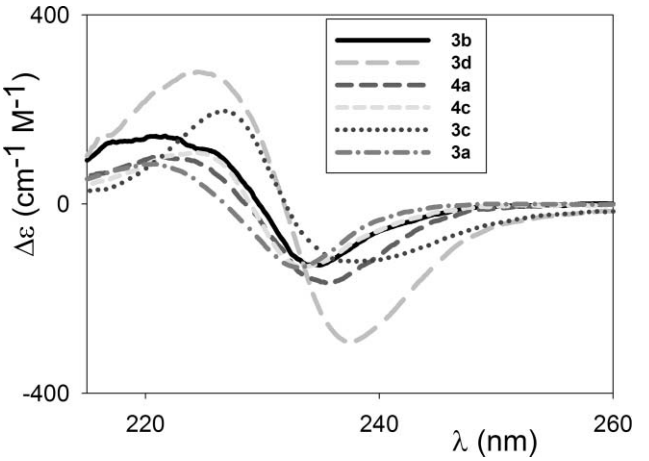

Fig. 4 CD spectra of macrocycles **3** and **4** (concentrations in the range $0.8–1.5 \times 10^{-6}$ M in EtOH).

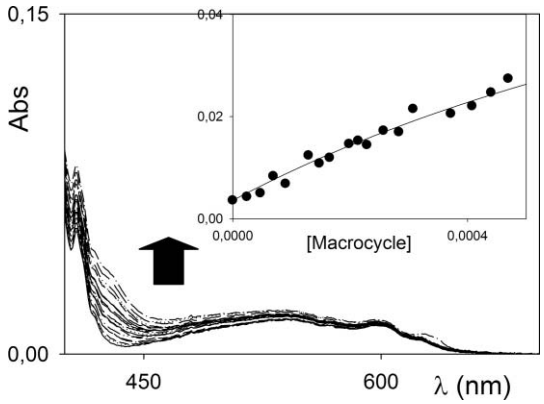

Fig. 5 Titration of C_{60} (5×10^{-5} M) with macrocycle **4c** ($0\text{-}5 \times 10^{-3}$ M) in toluene at 25 °C; inset: best fitting of the titration curve data at 437 nm with a 1 : 1 binding equation. See text and experimental section for details.

at 437 nm reach in both cases a similar value (ε = 1320 and 1450 M^{-1} cm^{-1} in the case of **4b** and **4c**, respectively). In the case of macrocycle **4c** the titration curve could be interpolated with good confidence with the equation derived for a 1 : 1 equilibrium[21] (Fig. 5, inset, and ESI†), giving a binding constant of 1100 M^{-1}. However, in the case of **4b** the shape of the titration profile and the very poor fitting with the 1 : 1 binding equation revealed that simultaneous equilibria with different stoichiometries are in place; the possibility, in the case of **4b**, of having two macrocycles endcapping one fullerene molecule, as an equilibrium in solution competing with the 1 : 1 binding stoichiometry, is suggested both by the molecular modeling (*vide infra*), and by the comparison with the behavior reported for calixarene and cyclodextrin receptors.[20h–l] The Hill equation has been recently used in association with complex binding events;[22] this equation gives two useful outputs: the average K_a for the binding events, and the Hill coefficient, a direct indication of the average number of species involved in the binding process.[23] Indeed, a good fitting could be obtained using the Hill equation, obtaining an average $K_a = 1250$ M^{-1}, and a Hill coefficient of 2.9 (Fig. 6).‡ Control experiments with the

‡ Although the sigmoidal shape of the binding isotherm, and the Hill coefficient higher than 1, seem to suggest positive cooperativity in the binding event,[32] recent reports have shown how the use of such an equation in order to prove positive cooperativity may be misleading (ref. 23). The Hill equation gives however an accurate value for the average K_a of all the binding processes involved.

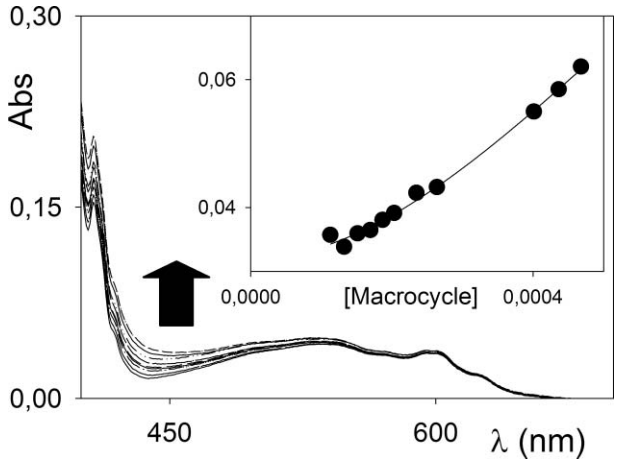

Fig. 6 Titration of C_{60} (10^{-4} M) with macrocycle **4b** ($0\text{-}5.0 \times 10^{-4}$ M) in toluene at 25 °C; inset: best fitting of the titration curve data at 437 nm with the Hill equation. See text and experimental section for details.

[2+2] macrocycle **3c**, or with fragments of the cyclic structures, such as terephthalic acid dimethyl ester or 2,2′-dimethoxy-1,1′-binaphthyl, instead, revealed no shift, outside the experimental error of the measurement, in the UV/Vis spectrum of C_{60} upon addition of the potential host (see ESI†).[24]

It is likely that a combination of nonspecific host–guest interactions (such as π–π stacking, but also van der Waals contacts between the polar -OCH_3 groups and the π-surface of the guest, *vide infra* molecular modeling) contributes to the overall stabilization of the complexes; the dependence of the binding on the size of the host ([3 + 3] *vs.* [2 + 2] or open fragments) resembles the mechanism of complexation of guests in the cavities of suitably-sized cyclodextrins.[25]

Molecular modeling

Molecular modeling was performed on the structures of compounds **4b** and **4c** in order to clarify the mechanism of C_{60} complexation and to estimate the final complexation energies. The method used for all the calculations was a semiempirical PM3 method, initially to optimize **3b** and **3c** structures and compare the results with the obtained crystal structures.[26] Theoretical minimum **3b** and **3c** were strikingly in accordance with the crystal structures (see ESI†), apart from a small deviation of planarity among the carboxyl group and the benzene ring observed in the computationally calculated structures.

In modeling both **4b** and **4c**, since they possess degrees of rotation around the ester linkages, particular care was applied in order to find all the different energy minima. This goal was achieved by performing short molecular dynamics on the obtained geometries followed by geometry optimization. The same approach was used for C_{60} complexes. Furthermore, complexation energy of 2 : 1 complexes macrocycle–C_{60} was estimated and results are reported below.

For **4b** several minima very close in energy (4 kcal mol^{-1} energy span) were found, associated with conformations all having a

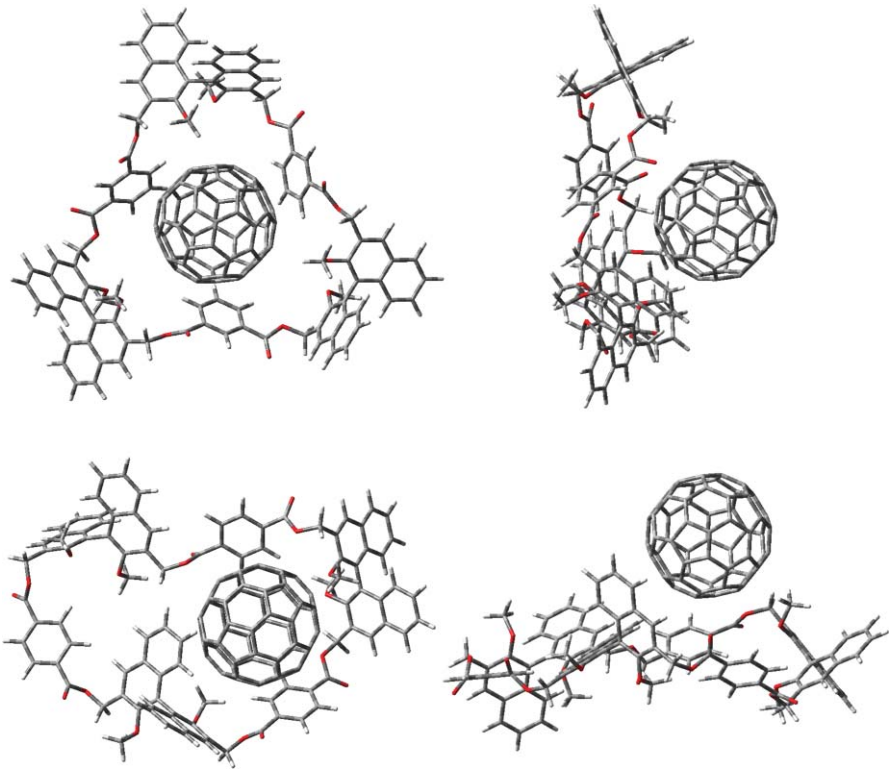

Fig. 7 Front and side view for the calculated minima C_{60}@**4b** (top), and for C_{60}@**4c** (bottom).

concave shape with local C_3 symmetry. These structures resemble a calixarene shape, in which each binaphthyl moiety has a methoxy group pointing into the cavity. For these conformations a complexation energy (ΔE) of 1 kcal mol^{-1} was estimated. The fullerene surface resides only 2.6 Å away from the closest hydrogen atom belonging to the three OMe groups (the ones pointing towards the cavity) of each binaphthyl moiety, these being the closest 'contact' atoms (Fig. 7). The three phenyl groups of the isophthalic spacers face toward the hosted molecule lying at a minimum distance of about 5.2 Å. In Fig. 8 is shown the geometry of the energy minimum of C_{60}@**4b**, in which it is evident that fullerene molecule can fit into the cavity. Surprisingly, the complexation energy of two molecules of **4b** with a C_{60} molecule turned out to be 3 kcal mol^{-1} (1.5 kcal mol^{-1} for each **4b** subunit); thus showing that the complexation of a second molecule of **4b** is more favorable with respect to the first. The optimized geometry (Fig. 8) shows that there is an interaction between the two adjacent **4b** rims.

The case of **4c** is different, as the conformer having minimum of energy is a collapsed structure more stable by about 9 kcal mol^{-1} with respect to the 'open' structure (see Fig. S13†). We can hence suppose that the structure of **4c** is to some extent more flexible with respect to **4b**; this could be due to the larger spacing offered by the *p*-substituted aromatic moieties that permit an easier rotation of the binaphthyls. The most stable complex observed of **4c** with C_{60} results from a partially collapsed structure (Fig. 7, bottom). This implies a non-optimal asymmetric complexation with only two methoxy groups interacting with the fullerene guest. In fact, the complexation energy is somewhat reduced to only 0.5 kcal mol^{-1}. In other words, the complexation energy of C_{60} is not sufficient to balance the energy requested to maintain the open structure. The calculated minima of two **4c** subunits with one of C_{60} is unfavorable for 14 kcal mol^{-1} thus suggesting that a 1 : 1 complex is predominant over a hypothetical 2 : 1 complex.

Conclusion

We have optimized conditions to achieve, in a one pot esterification reaction, the formation of chiral large macrocyclic receptors incorporating axially-chiral binaphthyl units. The introduction of ester functionalities ensures the required degree of flexibility and chemical inertness, making these substrates, once of suitable size, capable of recognition properties towards base-degradable, convex guest substrates such as C_{60}. The inclusion of small solvate molecules in the solid state points out that the enantioselective recognition of small organic species by these guests is worthwhile investigating. The deep understanding of the solution and solid state behaviour of these cyclic compounds is our driving force towards the design of improved cyclic species able to perform two ambitious goals: (a) function as enantioselective hosts for the detection of chiral fullerenes/carbon nanotubes; (b) assemble more specifically and strongly in the third dimension in order to generate helical, oriented organic nanotubes.

Experimental

All commercially available compounds were purchased from commercial sources and used as received. Compounds DPTS,[13] (*R*)-**1**,[12] **2d**,[27] **3a**,[11] **3c**,[11] **4a**[11] and **4c**[11] were prepared according to literature procedures. THF (Na) and CH_2Cl_2 (CaH_2) were dried

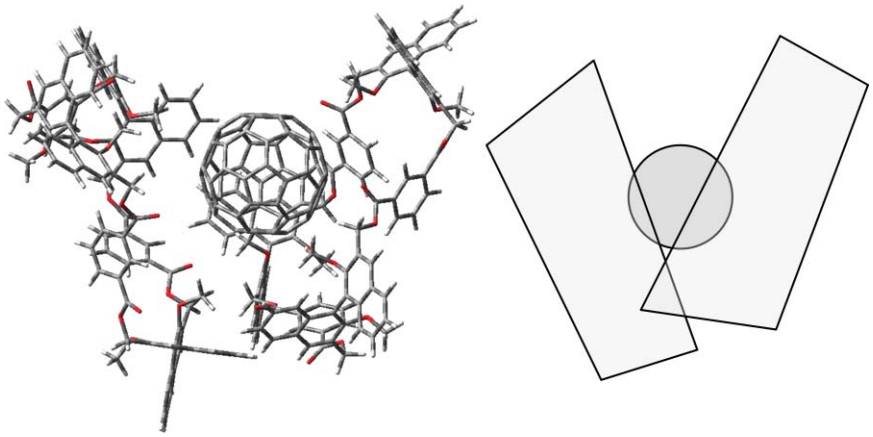

Fig. 8 Optimized geometry (left) and pictorial representation (right) for the complex between two molecules of **4b** and one of fullerene.

before use. Analytical thin layer chromatography was performed on silica gel, chromophore loaded, commercially available plates. Flash chromatography was carried out using silica gel (pore size 60 Å, 230–400 mesh). ^{1}H and ^{13}C NMR spectra were recorded from solutions in $CDCl_3$ on a 200 or 300 MHz spectrometer with the solvent residual proton signal or tetramethylsilane as a standard. The UV/Vis spectroscopic studies were recorded using commercially-available spectrophotometers. Mass spectra were recorded using an electrospray ionization instrument. Optical rotations were measured on a polarimeter with a sodium lamp ($\lambda =$ 589 nm) and are reported as follows: $[\alpha]_D^{rt}$ (c g (100 mL solvent)$^{-1}$). CD spectroscopy was performed using a commercially-available spectropolarimeter; spectra were recorded at 25 °C at a scanning speed of 50 nm min $^{-1}$ and were background corrected.

General procedure for the preparation of macrocycles 3 and 4

A solution of DICD (diisopropylcarbodiimide, 2.5 equivalents *vs.* diol and dicarboxylic acid) in a minimum amount of dry CH_2Cl_2 is added to a solution of the appropriate dicarboxylic acid (20–25 mM), (*R*)-**1** (20–25 mM), DPTS (0.9 equivalents) in dry CH_2Cl_2 under stirring and N_2 flow. The solution is stirred overnight, and then H_2O/ice (10 mL) is added. The aqueous phase is extracted with CH_2Cl_2 (3 ×), the organic phase is washed with H_2O (3 ×) and dried ($MgSO_4$). After evaporation of the organic phase to dryness, the products are purified by flash chromatography.

Macrocycles (*RR*)-3b and (*RRR*)-4b. From isophthalic acid (89 mg, 0.54 mmol), DICD (202 mg, 1.60 mmol), DPTSA–DMAP (166 mg, 0.535 mmol) and (*R*)-**1** (200 mg, 0.535 mmol). Purified by column chromatography (hexanes–EtOAc: 8/2) to yield **3b** (25 mg, 10%) and **4b** (7 mg, 3%) as white solids. (*RR*)-**3b**. $[\alpha]_D^{25}$ +22.8 (c 0.005 in CH_2Cl_2). ^{1}H NMR ($CDCl_3$, 300 MHz, 25 °C) $\delta = 8.66$ (s, 2H; phenyl), 8.34 (d, 4H; phenyl), 8.04 (s, 4H; binaphthyl), 7.83 (d, 4H; binaphthyl), 7.60 (t, 2H; phenyl), 7.37 (t, 4H; binaphthyl), 7.22 (t, 4H; binaphthyl), 7.08 (d, 4H; binaphthyl), 5.62 (dd, 4H; -CH_2OCO-), 3.24 (s, 12H; OMe). ^{13}C NMR ($CDCl_3$, 75 MHz, 25 °C) $\delta = 165.0$, 155.3, 134.3, 134.2, 131.6, 130.6, 130.2, 130.1, 128.7, 128.1, 126.8, 125.4, 125.1, 124.6, 63.2, 61.3. MS(ESI): m/z 1031.3 ([M + Na]$^+$, 100%). (*RRR*)-**4b**. $[\alpha]_D^{25}$ −9.7 (c 0.002 in CH_2Cl_2).^{1}H NMR ($CDCl_3$, 200 MHz, 25 °C) $\delta = 8.80$ (s, 3H; phenyl), 8.34 (d, 6H; phenyl), 8.08 (s, 6H; binaphthyl), 7.79 (d, 6H; binaphthyl), 7.59 (t, 3H; phenyl), 7.28 (t, 6H; binaphthyl), 7.19 (m, 12H; binaphthyl), 5.67 (bs, 12H; -CH_2OCO-), 3.29 (s, 9H; -OMe). ^{13}C NMR ($CDCl_3$, 75 MHz, 25 °C) $\delta = 165.4$, 156.0, 134.2, 134.1, 130.6, 130.5, 130.3 (Cq), 129.0 (CH), 128.7 (Cq), 128.0 (CH), 126.7 (CH), 125.5 (CH), 125.0 (CH), 124.0 (Cq), 63.2 (CH_2), 61.2 (OMe). MS(ESI): m/z 1535.6 ([M + Na]$^+$, 100%).

Macrocycle (*RR*)-3d. From **2d** (122 mg, 0.502 mmol), DICD (190 mg, 1.51 mmol), DPTSA–DMAP (156 mg, 0.502 mmol) and (*R*)-**1** (188 mg, 0.502 mmol). Purified by column chromatography (hexanes–CH_2Cl_2: 4/6) to yield **3d** (15 mg, 5%) as a white solid. $[\alpha]_D^{25}$ −84 (c 0.003 in CH_2Cl_2). ^{1}H NMR ($CDCl_3$, 300 MHz, 25 °C) $\delta =$ 8.38 (s, 4H; phenyl), 8.09 (d, 4H; phenyl), 8.00 (s, 4H; binaphthyl), 7.93 (d, 4H; binaphthyl), 7.84 (d, 4H; phenyl), 7.56 (t, 4H; phenyl), 7.46 (t, 4H; binaphthyl), 7.47 (t, 4H; binaphthyl), 7.38 (t, 4H; binaphthyl), 5.81 (d, 4H; -CH_2OCO-), 5.48 (d, 4H; -CH_2OCO-), 3.14 (s, 12H; OMe). ^{13}C NMR ($CDCl_3$, 75 MHz, 25 °C) $\delta = 167.1$, 156.5, 139.9, 134.8, 131.6, 131.1, 130.4, 129.7, 129.0, 128.9, 128.7, 128.1, 127.8, 126.9, 125.5, 124.9, 124.1, 65.8, 60.3. MS(ESI): m/z 1182.6 ([M + Na]$^+$, 100%).

UV/Vis titrations

Toluene (UV/Vis spectroscopic grade) was used. An analytical balance (with a precision of 10^{-4} g) was used to weight the samples for the stock solutions. Aliquots of these stock solutions were then taken *via* high precision syringes to prepare the cuvette samples for spectrophotometric analyses. The titration experiments were conducted as follows: to a stock solution of C_{60} (solution A) in MeCN, were added several aliquots of the host (solution B). Solution B is formed by the ligand at higher concentration dissolved in solution A, in order to maintain the guest always at the same, constant concentration.

In the case of a 1 : 1 binding isotherm, by employing a nonlinear fitting curve program, the plot of A against the metal concentration x was fitted by eqn (1), thus affording the value of the association constant K_a.

$$A = (\varepsilon_c - \varepsilon_s)\frac{k_a(C+x)+1-\left[\left[k_a(C+x)+1\right]^2-4k_a{}^2Cx\right]^{0.5}}{2k_a}+\varepsilon_s C \quad (1)$$

where A is the measured absorbance, x is the total concentration of titrant added, ε_c is the molar absorptivity of the complex, ε_s is the molar absorptivity of the substrate at the desired wavelength, which could be directly determined, C is the total concentration of the titrate (which is a constant quantity, usually the crown ether), and K_a is the association constant for the 1 : 1 complex.[21]

The data for titrations of **4b** with C_{60} (Fig. 6) were fitted to a general form of the Hill equation:

$$\Delta\text{Abs} = \Delta\text{Abs}_{max}\,[x]^n\,K_a/(1 + [x]^n\,K_a)$$

which can be conveniently rewritten in:

$$\Delta\text{Abs} = \Delta\text{Abs}_{max}\,[x]^n/[(1/K_a)^n + [x]^n] \quad (2)$$

Eqn (2) could be fitted employing a nonlinear fitting program according to the general equation: $f(x) = a^*x^b/(c^b + x^b)$, obtaining values of $a = \Delta\text{Abs}_{max}$, $b = n$ (the Hill coefficient), $c = 1/K_a$.

X-Ray crystallography

Diffraction data for **3b** and **3c** crystals have been collected at ambient temperature by means of an Enraf-Nonius CAD4 four circle diffractometer, working with graphite-monochromatized Mo-Kα X-radiation ($\lambda = 0.7107$ Å). Data reductions (including intensity integration, background, Lorentz and polarization corrections) were performed with the WinGX package.[28] Absorption effects were evaluated with the psi-scan method[29] and absorption correction was applied to the data: min./max. transmission factors were 0.895/0.987 and 0.872/0.959 for **3b** and **3c**, respectively. Crystal data are shown in the supporting information (Table S1†). Both crystal structures were solved by direct methods (SIR 97)[30] and refined by full-matrix least-square procedures on F^2 using all reflections (SHELXL97).[31] Anisotropic displacement parameters were refined for all non-hydrogen atoms. Hydrogens were placed at calculated positions with the appropriate AFIX instructions and refined using a riding model. CCDC 746582 and 746583.

Acknowledgements

Financial support from the University of Pavia, MIUR (PRIN 2004 "Ingegneria Cristallina di Materiali a Base Molecolare", and PhD studentship for MC), Regione Lombardia (INGENIO postdoctoral fellowship to CC) and Fondazione CARIPLO (2007-2009 "Self-Assembled Nanostructured Materials: A Strategy for the Control of Electrooptic Properties", DP) is gratefully acknowledged.

Notes and references

1 (*a*) D. T. Bong, T. D. Clark, J. R. Granja and M. R. Ghadiri, *Angew. Chem., Int. Ed.*, 2001, **40**, 988–1011; (*b*) C. Grave and A. D. Schlüter, *Eur. J. Org. Chem.*, 2002, 3075–3098; (*c*) Y. Yamaguchi and Z. Yoshida, *Chem.–Eur. J.*, 2003, **9**, 5430–5440; (*d*) D. Zhao and J. S. Moore, *Chem. Commun.*, 2003, 807–818; (*e*) S. Höger, *Chem.–Eur. J.*, 2004, **10**, 1320–1329; (*f*) W. Zhang and J. S. Moore, *Angew. Chem., Int. Ed.*, 2006, **45**, 4416–4439; (*g*) D. Pasini and M. Ricci, *Curr. Org. Synth.*, 2007, **4**, 59–80.

2 (*a*) M. R. Ghadiri, J. R. Granja and L. K. Buehler, *Nature*, 1994, **369**, 301–304; (*b*) W. S. Horne, N. Ashkenasy and M. R. Ghadiri, *Chem.–Eur. J.*, 2005, **11**, 1137–1144; (*c*) S. Leclair, P. Baillargeon, R. Skouta, D. Gauthier, Y. Zhao and Y. L. Dory, *Angew. Chem., Int. Ed.*, 2004, **43**, 349–353; (*d*) L. Fischer, M. Decossas, J.-P. Briand, C. Didierjean and G. Guichard, *Angew. Chem., Int. Ed.*, 2009, **48**, 1625–1628; (*e*) C. Reiriz, R. J. Brea, R. Arranz, J. L. Carrascosa, A. Garibotti, B. Manning, J. M. Valpuesta, R. Eritja, L. Castedo and J. R. Granja, *J. Am. Chem. Soc.*, 2009, **131**, 11335–11337; (*f*) See also: G. Dan Pantoş, P. Pengo and J. K. M. Sanders, *Angew. Chem., Int. Ed.*, 2007, **46**, 194–197.

3 (*a*) S. Höger, *Angew. Chem., Int. Ed.*, 2005, **44**, 3806–3808; (*b*) C. Giansante, P. Ceroni, M. Venturi, V. Balzani, J. Sakamoto and A. D. Schlüter, *Chem.–Eur. J.*, 2008, **14**, 10772–10781; (*c*) L. Shu, M. Mueri, R. Krupke and M. Mayor, *Org. Biomol. Chem.*, 2009, **7**, 1081–1092; (*d*) J. Sakamoto and A. D. Schlüter, *Eur. J. Org. Chem.*, 2007, (16), 2700–2712; (*e*) Y. Li and A. H. Flood, *Angew. Chem., Int. Ed.*, 2008, **47**, 2649–2652.

4 (*a*) B. Gong, *Acc. Chem. Res.*, 2008, **41**, 1376–1386; (*b*) A. J. Helsel, A. L. Brown, K. Yamato, W. Feng, L. Yuan, A. J. Clements, S. V. Harding, G. Szabo, Z. Shao and B. Gong, *J. Am. Chem. Soc.*, 2008, **130**, 15784–15785.

5 (*a*) J. Yang, M. B. Dewal, D. Sobransingh, M. D. Smith, Y. Xu and L. S. Shimizu, *J. Org. Chem.*, 2009, **74**, 102–110; (*b*) J. Yang, M. B. Dewal and L. S. Shimizu, *J. Am. Chem. Soc.*, 2006, **128**, 8122–8123.

6 (*a*) M. Oh and C. A. Mirkin, *Nature*, 2005, **438**, 651–654; (*b*) J. Heo, Y.-M. Jeon and C. A. Mirkin, *J. Am. Chem. Soc.*, 2007, **129**, 7712–7713; (*c*) T. Tu, T. Maris and J. D. Wuest, *Cryst. Growth Des.*, 2008, **8**, 1541–1546.

7 For general reviews, see:(*a*) L. Pu, *Chem. Rev.*, 1998, **98**, 2405–2494; (*b*) J. M. Brunel, *Chem. Rev.*, 2005, **105**, 857–898; (*c*) For selected recent examples, see: S. Tosaki, K. Hara, V. Gnanadesikan, H. Morimoto, S. Harada, M. Sugita, N. Yamagiwa, S. Matsunaga and M. Shibasaki, *J. Am. Chem. Soc.*, 2006, **128**, 11776–11777; (*d*) V. Rauniyar and D. G. Hall, *Synthesis*, 2007, (21), 3421–3426, DOI: 10.1055/s-2007-983832; (*e*) B. Maciá Ruiz, K. Geurts, M. A. Fernández-Ibáñez, B. ter Horst, A. J. Minnaard and B. L. Feringa, *Org. Lett.*, 2007, **9**, 5123–5126; (*f*) B. Olenyuk, J. A. Whiteford and P. J. Stang, *J. Am. Chem. Soc.*, 1996, **118**, 8221–8230; (*g*) C. Coluccini, A. Castelluccio and D. Pasini, *J. Org. Chem.*, 2008, **73**, 4237–4240; (*h*) L. Ma, D. J. Mihalcik and W. Lin, *J. Am. Chem. Soc.*, 2009, **131**, 4610–4612; (*i*) Y. Zhu, N. Gergel, N. Majumdar, L. R. Harriott, J. C. Bean and L. Pu, *Org. Lett.*, 2006, **8**, 355–358; (*j*) G. Koeckelberghs, T. Verbiest, M. Vangheluwe, L. De Groof, I. Asselberghs, I. Picard, K. Clays, A. Persoons and C. Samyn, *Chem. Mater.*, 2005, **17**, 118–121.

8 (*a*) A. S. Droz, U. Neidlein, S. Anderson, P. Seiler and F. Diederich, *Helv. Chim. Acta*, 2001, **84**, 2243–2289; (*b*) A. Bähr, A. S. Droz, M. Püntener, U. Neidlein, S. Anderson, P. Seiler and F. Diederich, *Helv. Chim. Acta*, 1998, **81**, 1931–1963.

9 T. Kawase, T. Nakamura, K. Utsumi, K. Matsumoto, H. i. Kurata and M. Oda, *Chem.–Asian J.*, 2008, **3**, 573–577.

10 (*a*) J. Lin, H.-C. Zhang and L. Pu, *Org. Lett.*, 2002, **4**, 3297–3300; (*b*) Z.-B. Li, J. Lin, H.-C. Zhang, M. Sabat, M. Hyacinth and L. Pu, *J. Org. Chem.*, 2004, **69**, 6284–6293; (*c*) L. Z.-B. Li, J. Lin and L. Pu, *Angew. Chem., Int. Ed.*, 2005, **44**, 1690–1693; (*d*) J. Heo and C. A. Mirkin, *Angew. Chem., Int. Ed.*, 2006, **45**, 941–944In an interesting case, the coupling of resolved, optically active binaphthols such as (*R*)-**1** with optically-active 1,2-diphenylethylenediamine furnished the [2+2] macrocycle only when one enantiomer of the diamine was used, see:; H. Brunner and H. Schliessing, *Angew. Chem., Int. Ed. Engl.*, 1994, **33**, 125–126.

11 Part of this work has been the subject of a preliminary communication:M. Ricci and D. Pasini, *Org. Biomol. Chem.*, 2003, **1**, 3261–3262.

12 H. T. Stock and R. M. Kellogg, *J. Org. Chem.*, 1996, **61**, 3093–3105.

13 J. S. Moore and S. I. Stupp, *Macromolecules*, 1990, **23**, 65–70.

14 A. W. Freeman and J. M. J. Fréchet, *Org. Lett.*, 1999, **1**, 685–687.

15 For a review on dynamic covalent chemistry, see: (*a*) S. J. Rowan, S. J. Cantrill, G. R. L. Cousins, J. K. M. Sanders and J. F. Stoddart, *Angew. Chem., Int. Ed.*, 2002, **41**, 898–952We speculate one possible rationalization of such behavior (that is: the absence of template effects, of dynamic covalent behavior, yet isolated yields which, in some cases, are far superior with respect to other conventional methods in which all reagents and products are soluble in the reaction solvent) can be found in the precipitation assisted macrocyclization concept. For an example, see:; W. Zhang and J. S. Moore, *J. Am. Chem. Soc.*, 2004, **126**, 12796.

16 Variable temperature ^{1}H NMR studies, conducted on the macrocycle **4c**, showed, with the decrease of temperature, a splitting of the resonances in a well defined AB quartet. This indicates that the conformational preference present for the larger macrocycles at room temperature is not accessible at lower temperatures. See ref.11 for details.

17 (*a*) N. Chronakis, T. Brandmüller, C. Kovacs, U. Reuther, W. Donaubauer, F. Hampel, F. Fischer, F. Diederich and A. Hirsch, *Eur. J. Org. Chem.*, 2006, 2296–2308; (*b*) U. Reuther, T. Brandmüller, W. Donaubauer, F. Hampel and A. Hirsch, *Chem.–Eur. J.*, 2002, **8**, 2261–2273.

18 (*a*) G. Gattuso, S. Menzer, S. A. Nepogodiev, J. F. Stoddart and D. J. Williams, *Angew. Chem., Int. Ed. Engl.*, 1997, **36**, 1451–1454; (*b*) P. R. Ashton, S. J. Cantrill, G. Gattuso, S. Menzer, S. A. Nepogodiev, A. N. Shipway, J. F. Stoddart and D. J. Williams, *Chem.–Eur. J.*, 1997, **3**, 1299–1314.

19 (*a*) C. Rosini, S. Superchi, H. W. I. Peerlings and E. W. Meijer, *Eur. J. Org. Chem.*, 2000, 61–71; (*b*) it should be emphasized that even large variations in the maximum value of the low energy component of the couplet correspond to little changes in the dihedral binaphthyl angle.

20 For recent reviews, see: (*a*) T. Kawase and H. Kurata, *Chem. Rev.*, 2006, **106**, 5250–5273; (*b*) K. Tashiro and T. Aida, *Chem. Soc. Rev.*, 2007, **36**, 189–197; (*c*) for examples of receptors for fullerenes: Y. Yamaguchi, S. Kobayashi, N. Amita, T. Wakamiya, Y. Matsubara, K. Sugimoto and Z. Yoshida, *Tetrahedron Lett.*, 2002, **43**, 3277–3280; (*d*) H.-Y. Gong, X.-H. Zhang, D. X. Wang, H.-W. Ma, Q.-Y. Zheng and M.-X. Wang, *Chem.–Eur. J.*, 2006, **12**, 9262–9275; (*e*) S.-Q. Liu, D.-X. Wang, Q.-Y. Zheng and M.-X. Wang, *Chem. Commun.*, 2007, 3856–3858; (*f*) Y.-Y. Zhu, C. Li, G.-Y. Li, X.-K. Jiang and Z.-T. Li, *J. Org. Chem.*, 2008, **73**, 1745–1751; (*g*) J. Effing, L. Jonas, L. Jullien, T. Plesnivy, H. Ringsdorf, F. Diederich, C. Thilgen and D. Weinstein, *Angew. Chem., Int. Ed. Engl.*, 1992, **31**, 1599–1602; (*h*) Z.-I. Yoshida, H. Yakekuma, S.-I. Takekuma and Y. Matsubara, *Angew. Chem., Int. Ed. Engl.*, 1994, **33**, 1597–1599; (*i*) J. L. Atwood, M. J. Barnes, M. G. Gardiner and C. L. Raston, *Chem. Commun.*, 1996, 1449–1450; (*j*) E. Huerta, G. A. Metselaar, A. Fragoso, E. Santos, C. Bo and J. de Mendoza, *Angew. Chem., Int. Ed.*, 2007, **46**, 202–205; (*k*) A. Ikeda, T. Hatano, S. Shinkai, T. Akiyama and S. Yamada, *J. Am. Chem. Soc.*, 2001, **123**, 4855–4856; (*l*) T. Kawase, K. Tanaka, H. R. Darabi and M. Oda, *Angew. Chem., Int. Ed.*, 2003, **42**, 1624–1628; (*m*) Y. Shoji, K. Tashiro and T. Aida, *J. Am. Chem. Soc.*, 2006, **128**, 10690–10691; (*n*) G. Dell'Anna, R. Annunziata, M. Benaglia, G. Celentano, F. Cozzi, O. Francesconi and S. Roelens, *Org. Biomol. Chem.*, 2009, **7**, 3871–3877.

21 J. R. Long and R. S. Drago, *J. Chem. Educ.*, 1982, **59**, 1037–1089.

22 (*a*) E. M. Pérez, L. Sánchez, G. Fernández and N. Martín, *J. Am. Chem. Soc.*, 2006, **128**, 7172–7173; (*b*) G. Fernández, L. Sánchez, E. M. Pérez and N. Martín, *J. Am. Chem. Soc.*, 2008, **130**, 10674–10683.

23 The use of the Hill equation, and of the Hill coefficient in particular, as an interaction coefficient reflecting the extent of cooperativity, with a maximum value equal to the number of binding sites, has been recently discussed: G. Ercolani, *J. Am. Chem. Soc.*, 2003, **125**, 16097–16103S. ee also:; J. Hamacek and C. Piguet, *J. Phys. Chem. B*, 2006, **110**, 7783–7792.

24 Experiments in toluene-d_8, with both control compound **3c** and guest macrocycle **4c** and C_{60} (300 MHz) revealed very small shifts in the guest counterpart upon complexation, at the level of the measurement statisctical error (see Fig. S2 and S3†). Qualitatively similar results in toluene have been reported for other fullerene receptors (see ref. 20*f* and 20*p*). CD spectroscopy performed in toluene, with **4c** in the presence of C_{60}, at the low concentration needed to run the experiment in the CD spectropolarimeter ($5\ 10^{-6}$ M) revealed no induced CD effect in any of the corresponding band of the C_{60} chromophore, nor any possibility to develop CD spectroscopy as a tool complementary to UV/Vis spectroscopy for the detection of the guest. See also: A. Moletti, C. Coluccini, D. Pasini and A. Taglietti, *Dalton Trans.*, 2007, (16), 1588–1592, and ref. 18*o*. Experiments run with 1 : 1 mixtures of macrocycle **4c** and C_{60}, to evidence complex formation in the gas phase by ESI MS, in the positive mode, revealed, as in reference 20*p*, peaks related only to the macrocyclic component.

25 M. V. Rekharsky and Y. Inoue, *Chem. Rev.*, 1998, **98**, 1875–1917.

26 (*a*) P. Mukherjee, A. Ray, A. K. Bauri and S. Bhattacharya, *J. Mol. Liq.*, 2009, **148**, 51–57; (*b*) S. Bhattacharya, S. K. Nayak, S. Chattopadhyay, M. Banerjee and A. K. Mukherjee, *J. Phys. Chem. B*, 2003, **107**, 13022–13028.

27 1,1′-Diphenyl-3,3′-dicarboxylic acid was prepared by hydrolysis (Et-ONa/EtOH) of the corresponding diethylester (prepared as reported in: J. Hassan, V. Penalva, L. Lavenot, C. Gozzi and M. Lemaire, *Tetrahedron*, 1998, **54**, 13793–13804.

28 L. J. Farrugia, *J. Appl. Crystallogr.*, 1999, **32**, 837–838.

29 A. C. T. North, D.C. Phillips and F. S. Mathews, *Acta Crystallogr., Sect. A: Cryst. Phys., Diffr., Theor. Gen. Crystallogr.*, 1968, **24**, 351–359.

30 A. Altomare, M. C. Burla, M. Camalli, G. L. Cascarano, C. Giacovazzo, A. Guagliardi, A. G. G. Moliterni, G. Polidori and R. Spagna, *J. Appl. Crystallogr.*, 1999, **32**, 115–119.

31 G. M. Sheldrick, *SHELX97 Programs for Crystal Structure Analysis*, University of Göttingen, Germany, 1997.

32 L. D. Byers, *J. Chem. Educ.*, 1977, **54**, 352–354.